

# Conditional preparation of single photons for scalable quantum-optical networking

Alfred B. U'Ren, Christine Silberhorn, Konrad Banaszek, and Ian A. Walmsley  
Clarendon Laboratory, Oxford University, Parks Road, Oxford, OX1 3PU, England.

(Dated: October 31, 2018)

A fundamental prerequisite for the implementation of linear optical quantum computation is a source of single-photon wavepackets capable of high-visibility interference in scalable networks. These conditions can be met with micro-structured waveguides in conjunction with ultra-short classical timing pulses. By exploiting a novel type-II phasematching configuration we demonstrate a waveguided single photon source exhibiting a conditional *detection* efficiency exceeding 51% (which corresponds to a *preparation* efficiency of 85%) and extraordinarily high detection rates of up to  $8.5 \times 10^5$  coincidences/[s-mW].

PACS numbers: 42.50.Ar, 03.67.Lx

Single photons provide an important bridge between classical and non-classical physics. For example, it is possible to define a single-photon wavefunction that has exactly the same form as the classical electromagnetic field[? ], yet the quadrature phase-space representations of the state can be singular or non-positive[2]. Apart from fundamental interest, the ability to generate single-photon wavepackets in a scalable manner is a prerequisite for the further development of quantum-enhanced technologies. Recent progress in quantum information processing highlights the necessity for a reliable single photon source. At the heart of such novel proposals is quantum interference, which necessitates photonic wavepackets exhibiting well-defined photon number and a well-defined modal character. Thus, modal distinguishability hinders the implementation of linear optical quantum computation [3, 4, 5] and indeed of all schemes relying on interference between single photons from multiple sources[6] such as teleportation[7, 8], entanglement swapping[9] and networking via quantum repeaters[10]. Furthermore, single photon emission in well-defined modes permits efficient fiber coupling, crucial for long-haul quantum cryptography and communication[11].

Two distinct approaches for generating single photons are currently being pursued: deterministic sources of single photons emitted on-demand, and spontaneous sources based on photon-pair generation where a single photon is prepared by detection of the conjugate pair member. Sources based on single vacancy centers[13], quantum dots[14, 15, 16], atoms in cavities[17] and molecular emission[18] emit photons deterministically, and often rely on intricate experimental setups (e.g. cryostatic cooling). For solid-state sources, however, it remains challenging to control the emission modes, resulting in poor interference, poor fiber-coupling and low detection efficiencies. This in turn leads to a random selection of collected photons. In the process of parametric down-conversion (PDC), on the other hand, photon pair emission occurs randomly but the presence of a single photon can be determined by the detection of its sibling. It is nevertheless difficult to collect the entire photon sample from bulk crystals[19, 20] due to the relatively

complicated spatial emission pattern. PDC from quasi phasematched non-linear waveguides has recently been shown, however, to exhibit emission in controlled modes defined by the guide[21, 22, 23, 24]. Accurate spatial mode definition leads to efficient optical fiber coupling and to much improved conditional detection rates as well as high-visibility interference. A fundamental requirement for high-fidelity conditional preparation of single photons based on waveguided PDC is efficient pair-splitting, which is realized here through a nonlinear interaction producing orthogonally-polarized (and therefore spatially separable) photon pairs.

The difficulty in generating orthogonally polarized PDC light in a waveguided  $\chi^{(2)}$  interaction is that existing waveguide structures are commonly designed to take advantage of the high  $d_{33}$  nonlinearities of LiNbO<sub>3</sub> and KTiOPO<sub>4</sub> (KTP) which implies the use of type-I phasematching yielding same-polarization PDC photon pairs. Since waveguided PDC additionally implies that both PDC photons in a given pair occupy a waveguide-supported spatial mode, it is challenging to split the pairs. For common  $\chi^{(2)}$  materials such as periodically poled LiNbO<sub>3</sub> (PPLN), waveguiding supports only one polarization. Thus, to date, quantum optical experiments making use of nonlinear waveguides have employed this type of phasematching[21, 22, 23, 24, 25]. We have designed a type-II PDC interaction in a periodically poled KTP waveguide which leads to easily separable (by means of their polarization) photon pairs. In such a phasematching configuration (utilizing the  $\chi^{(2)}$  element  $d_{24}$ ), a horizontally-polarized ultraviolet photon spontaneously decays into two infrared photons, horizontally and vertically polarized.

Our experimental apparatus is depicted in Fig. 1. The output of a mode-locked titanium sapphire laser (100fs pulse duration, 87MHz repetition rate) is directed to a 2mm-long  $\beta$ -barium-borate crystal yielding pulses centered at 400.5nm, whose bandwidth is restricted by an interference filter with a FWHM of 2nm. This ultraviolet beam (power measured before coupling was  $15\mu\text{W}$ ) is focused using a 10X microscope objective into the input face of a 12mm-long periodically poled z-cut KTP-waveguide (with  $8.7\mu\text{m}$  grating period). The wave-

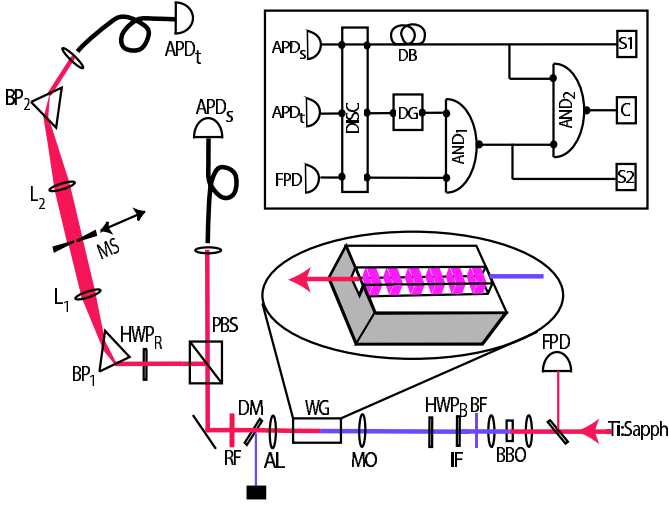


FIG. 1: Experimental apparatus with photon-counting electronics, including logic elements used for time-gating shown in inset. A quasi-phase-matched nonlinear waveguide is set up to produce orthogonally-polarized photon pairs via type-II downconversion. A polarization beam splitter divides the photon pair sample into two modes (trigger and signal) one of which (trigger) is subjected to spectral filtering and to post-detection time-gating (see inset) while the signal mode is directly detected. FPD: fast photodiode; BBO: 2mm  $\beta$ -barium-borate doubling crystal; BF: BG-39 Schott colored filter, IF: narrow-band pass filter, HWP<sub>B</sub>: half waveplate set to flip polarization; MO: 10X microscope objective; WG: 12mm long KTiOPO<sub>4</sub> waveguide with  $8.7\mu\text{m}$  period; AS: AR coated  $f=8\text{mm}$  aspheric lens; DM: blue-reflecting, red-transmitting dichroic mirror; RF: AR-coated RG-665 Schott colored filter; HWP<sub>R</sub> AR-coated halfwave plate; PBS: polarizing beam splitter; BP<sub>1</sub> and BP<sub>2</sub>: Brewster-angle SF-10prism; L<sub>1</sub> and L<sub>2</sub>:  $f = 10\text{cm}$  AR-coated lens; MS: translatable slit; APD<sub>t</sub>: trigger fiber-coupled avalanche photodiode (APD) from Perkin-Elmer; APD<sub>s</sub>: signal APD; INV: pulse inverter; DISC: pulse discriminator; DB: electronic variable delay line; DG: electronic delay generator (Stanford research DG-535); AND<sub>1</sub> and AND<sub>2</sub>: NIM AND gates; S<sub>1</sub>, S<sub>2</sub> and C: pulse counters.

uide output is collimated and the remaining ultraviolet is filtered out from the PDC signal. The photon pairs are subsequently split by a polarizing beam splitter and the horizontally polarized signal mode is coupled by a multi-mode fiber to a commercial silicon-based avalanche photodiode (APD). The trigger channel (vertical polarization) is subjected to a low-loss prism spectrometer comprised of two SF-10 Brewster angle prisms and two  $f = 10\text{cm}$  lenses; a motorized slit of adjustable width is placed at the Fourier plane whose position is computer-controlled. The resulting trigger mode is similarly launched into a fiber-coupled APD. The slit position is calibrated by transmitting a titanium sapphire beam through the prism setup into a spectrometer, where a linear extrapolation was made for wavelengths outside the laser bandwidth. To implement time-gating, a small percentage of the laser power is directed to a fast photo-

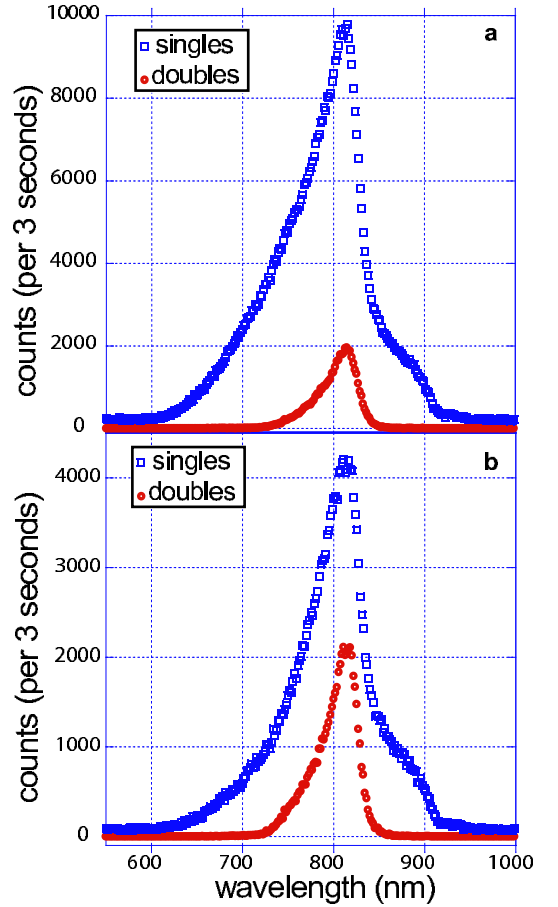


FIG. 2: Spectrally resolved parametric downconversion. (a) Frequency-resolved singles (trigger) and coincidence counts without time-gating. (b) Frequency-resolved singles (trigger) and coincidence counts with time-gating. Note that the maximum conditional detection efficiency increases from 20.4% to 50.5% upon activation of time-gating.

diode (1ns rise-time). The diode signal is amplified and discriminated producing a train of 3ns duration pulses which is delayed (with an electronic delay generator) and combined at an AND gate with the discriminated trigger output. A second AND gate comparing the time-gated and non-gated signals registers when both inputs arrive simultaneously (to within 3ns).

Waveguided PDC leads to several key advantages: it increases source brightness and enables conditional preparation efficiencies limited only by detector losses while attaining accurate spatio-temporal modal control. Despite the fact that in KTP the  $d_{24}$  element is considerably smaller in magnitude than those elements yielding type I PDC ( $d_{33}$  and  $d_{31}$ ), it is possible to obtain a remarkably high production rate of type-II PDC photon pairs since the nonlinear gain exhibits a quadratic dependence on the guide length (rather than linear dependence for bulk crystals). In our experiment one of the polarizations is regarded as a trigger, while we attempt to collect all photons in the orthogonal polarization (signal). In the

limit of unit detector quantum efficiency together with vanishing optical losses and perfectly-suppressed background, a trigger detection heralds the presence of a single photon in the signal arm. Such conditional detection is characterized by an efficiency given by the ratio of coincidence (trigger and signal) to singles (trigger) detection rates. The source brightness, given by the coincidence rate per unit pump power, is an additional important measure of source performance, specifically in the context of concatenating multiple waveguides for quantum-optical networking.

We encountered two important sources of background photons produced by our waveguide. If not suppressed, such uncorrelated light is a serious limitation to the conditional detection efficiency. First, the quasi phase-matched grating needed for type-II PDC (with  $8 - 10\mu\text{m}$  period) also supports type-I PDC, resulting from the  $\chi^{(2)}$  elements  $d_{33}$  and  $d_{31}$ , producing same-polarization pairs which do not contribute to coincidence events and thus reduce the conditional detection efficiency. Fortunately, the various phasematched processes in the waveguide are spectrally distinct; indeed, we verified that a band-pass filter in the path of the ultraviolet pump can suppress type-I interactions. Second, the waveguide produces uncorrelated fluorescence photons, with an intensity comparable to that of PDC. The observed fluorescence is related to gray-tracking in KTP due to color-center formation[26] and has been observed in PDC from bulk periodically poled material[27]. While in a waveguide a substantial fraction of the fluorescence is emitted into the supported modes, we found that the fluorescence and PDC signals exhibit certain features that can be exploited to differentiate between them. By direct measurement we determined that the fluorescence spectrum is considerably wider than that of PDC (130nm versus 50nm 1/e full width). By filtering out frequencies at which PDC is not present, fluorescence is suppressed without appreciably reducing the PDC photon sample. Moreover, while PDC events occur within the femtosecond pump pulse window, fluorescence is emitted over much longer timescales. Therefore, gating in time with respect to the pump pulse train leads to further fluorescence suppression.

An experimental run consists of the recording of singles and coincidence detection rates as a function of the slit position. A slit width of  $40\mu\text{m}$  maximizes the transmitted signal at the highest spectral resolution (about 2nm). Data was taken with and without time-gating, as shown in Fig. 2. The maximum coincidence to singles ratio (i.e. the conditional detection efficiency) increases from 20.4% to 51.5% upon activation of time-gating. If the heralded single photons are prepared for a subsequent experiment, rather than detected directly, the preparation efficiency does not include the signal detection loss, which together with imperfect fiber coupling is the highest source of loss (detector specifications indicate 60% quantum efficiency at 800nm, measured fiber coupling efficiencies were  $> 90\%$  while all other optics incur negligible loss). For a quantum efficiency of 60%, a 51.5% con-

ditional detection efficiency corresponds to a preparation efficiency of single photons of close to 85%. The latter means that we can ascertain the presence of a single photon in a well-defined spatio-temporal mode with an 85% fidelity. Furthermore, annealing the color centers, e.g. by heating the waveguide[26], may suppress the remaining fluorescence and lead to nearly ideal single-photon preparation.

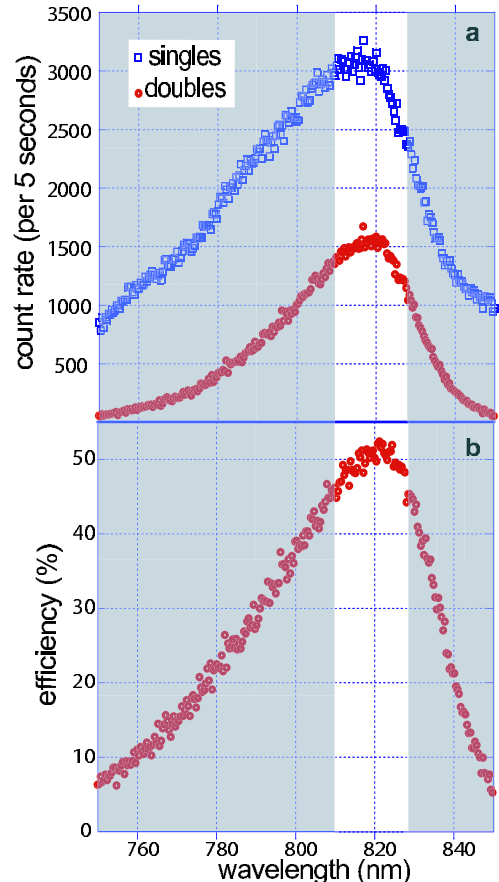


FIG. 3: Conditional detection efficiency for optimized source brightness. This figure shows spectrally-resolved coincidences and singles counts in the region of the coincidences peak. The non-shaded band indicates the location and width (corresponding to a 17nm spectral transmission window) of the pump spectrometer slit yielding the highest brightness ( $8.5 \times 10^5$  coincidences/[s·mW]) at the maximum conditional detection efficiency (51%). (a) Depicts the frequency-resolved coincidence and singles (trigger) detection rates (b) Depicts the conditional detection efficiency (given by the ratio of coincidence to singles counts).

In a second experiment, we optimized the source brightness in order to maximize optical throughput while retaining a high efficiency by adjusting the slit position and width, resulting in a 17nm transmission window. For a 300s integration time, we observed  $7.46 \times 10^5$  trigger,  $1.15 \times 10^7$  signal and  $3.81 \times 10^5$  coincidence counts (the calculated accidental coincidence rate is  $< 330$  counts) corresponding to a brightness of

$8.5 \times 10^5$  coincidences/(s·mW). For comparison with our spectrally-resolved measurements, Fig. 3 shows experimental data close to the coincidence peak; the non-shaded band indicates the slit position and width corresponding to simultaneous brightness and efficiency maximization. We have thus shown the experimental realization of high-fidelity conditional preparation of fiber-coupled single photons generated by a femtosecond-pulse pumped waveguide (in a micro-structured nonlinear optical array) based on orthogonally-polarized parametric downconversion photon pair generation from a periodically poled  $\text{KTiOPO}_4$  nonlinear waveguide[12]. The use of waveguiding leads to a high probability of photon pair generation which translates for our experiment into an extraordinarily high detection rate and a remarkable conditional efficiency. Such single photons are characterized by an ultrashort wavepacket with a broad spectral bandwidth. Furthermore, the use of an ultrashort pump pulse train constrains emission times to within a femtosecond-duration window, crucial for applications requiring synchronized emission from multiple sources.

To our knowledge, the best previously reported ratio obtained with CW-pumped PDC from a  $\beta$ -barium-borate crystal and collected with single-mode fibers was 28.6% at a brightness of 775 counts/(s·mW)[28]. The use of a CW pump in this experiment implies that there is not a classical timing signal for synchronization of multiple sources. Experiments aimed at determining the quantum efficiency of single-photon detectors have re-

ported high coincidence to singles ratios[29] when corrected for optical losses; however, photons in the signal arm lacked modal definition, limiting the potential for usable conditionally-prepared single photons. We believe that our higher brightness arises from accurate modal definition at the source, leading to efficient fiber-coupling of the whole photon sample. In contrast, for bulk crystal PDC, mode definition is only possible *a posteriori* (e.g. with irises or fibers).

Further development of our source could include modal engineering of the conditionally-prepared photon states to yield well-defined pure photon-number states (i.e. Fock states) and arbitrary superposition wavepackets[30, 31, 32]. Mode-matching into single-mode fibers should be straightforward given that the waveguide exhibits accurate spatial mode control. Precise timing together with high brightness paves the road towards concatenation of multiple waveguides in integrated quantum-optical networks. Thus our observed high brightness together with the use of an ultra-short pump, leads to source scalability by utilizing multi-waveguide chips. In addition, utilizing a higher pump power such high brightness permits the generation of higher-occupancy Fock states at experimentally-usable production rates. In conclusion, our source is an ideal building block for quantum information applications offering compatibility with all-fiber systems, while room-temperature operation makes it a convenient alternative to solid-state sources.

- 
- [1] I. Bialynicki-Birula, Prog. in Opt. **36**, 245 (1996)
- [2] A.I. Lvovsky *et al.*, Phys. Rev. Lett. **87**, 050402 (2001).
- [3] E. Knill, R. LaFlamme and G.J. Milburn, Nature **409**, 46 (2001).
- [4] T.C. Ralph, A.G. White, W.J. Munro and G.J. Milburn, Phys. Rev. A **65**, 012314 (2001).
- [5] T.B. Pittman, M.J. Fitch, B.C. Jacobs and J.D. Franson, quant-ph/0303095 (2003).
- [6] A.B. U'Ren, K. Banaszek and I.A. Walmsley, Quantum Information and Computation **3**, 480 (2003).
- [7] D. Bouwmeester *et al.*, Nature **390**, 575 (1997).
- [8] D. Boschi, S. Branca, F. De Martini, L. Hardy and L. Popescu, Phys. Rev. Lett. **80**, 1121 (1998).
- [9] J.W. Pan, D. Bouwmeester, H. Weinfurter and A. Zeilinger, Phys. Rev. Lett. **80**, 3891 (1998).
- [10] H.J. Briegel, W. Dür, J.I. Cirac and P. Zoller, Phys. Rev. Lett. **81**, 5932 (1998).
- [11] See for example review: N. Gisin, G.G. Ribordy, W. Tittel and H. Zbinden, Rev. of Mod. Phys. **74**, 145 (2002)
- [12] M.G. Roelofs, A. Suna, W. Bindloss and J.D. Bierlein, J. Appl. Phys. **76**, 4999 (1994).
- [13] C. Kurtsiefer, S. Mayer, P. Zarda and H. Weinfurter, Phys. Rev. Lett. **85**, 290 (2000).
- [14] P. Michler *et al.*, Science **290**, 2282 (2000).
- [15] Z. Yuan *et al.* Science **295**, 102 (2002).
- [16] C. Santori, D. Fattal, J. Vuckovic and Y. Yamamoto, Nature **419**, 594 (2002).
- [17] A. Kuhn, M. Hennrich and G. Rempe, Phys. Rev. Lett. **89**, 067901 (2002).
- [18] B. Lounis and W.E. Moerner, Nature **407**, 491 (2000).
- [19] M. Barberi, F. De Martini, G. Di Nepi and P. Mataloni, quant-ph/0303018, (2003).
- [20] E. Waks, E. Diamanti and Y. Yamamoto, quant-ph/0308055 (2003).
- [21] K. Banaszek, A.B. U'Ren and I.A. Walmsley, Opt. Lett. **26**, 1367 (2001).
- [22] H. Tanzilli *et al.*, Electron. Lett. **37**, 26 (2001).
- [23] K. Sanaka, K. Kawahara and T. Kuga, Phys. Rev Lett. **86**, 5620 (2001).
- [24] M.C. Booth *et al.*, Phys. Rev. A **66**, 023815 (2002).
- [25] M. E. Anderson, M. Beck, M. G. Raymer and J. D. Bierlein, Opt. Lett., **20**620 (1995).
- [26] B. Boulanger, *et al.*, IEEE J. Quant. Elect. **35**, 281 (1999).
- [27] C.E. Kuklewicz, M. Fiorentino, G. Messin, F.N.C Wong and J.H. Shapiro, quant-ph/0305092, (2003).
- [28] C. Kurtsiefer, M. Oberparleiter and H. Weinfurter, Phys. Rev. A **64**, 023802 (2001).
- [29] P.G. Kwiat, A.M. Steinberg and R.Y. Chiao, Phys. Rev. A **48**, R867 (1993).
- [30] W.P. Grice, A.B. U'Ren and I.A. Walmsley, Phys. Rev. A **64**, 063815 (2001).
- [31] M. Dakna, J. Clausen, L. Knöll and D.G. Welsch, Phys. Rev. A **59**, 1658 (1999).
- [32] D.T. Pegg, L.S. Phillips and S.M. Barnett, Phys. Rev. Lett. **81**, 1604 (1998).